Powder Metallurgy, *43(1), 37-42*.

A Robustness Simulation of Water Atomization

Bjarne Bergquist[1] and Torsten Ericsson[2]

[1.] *Currently at the Division of Quality Technology and Statistics, Dept. for Business Administration and Social Sciences, Luleå tekniska universitet, SE 971 87 Luleå, Sweden, formerly at the Division of Engineering Materials, Dept. of Mechanical Engineering, Linköpings universitet, SE 581 83 Linköping, Sweden*

[2.] *Division of Engineering Materials, Dept. of Mechanical Engineering, Linköpings universitet, SE 581 83 Linköping, Sweden*

1. Abstract

One of the main goals of water atomization is to keep the powder size distribution in close ranges. The process is difficult to monitor, and thus the state of today's process control is poor.

To investigate the process, both a laboratory scale and an industrial-scale atomization-facility were modeled, with focus on melt and thermal flow.

Results show that metal temperature is important if stable particle sizes from batch to batch should be obtained.

Key words: Simulation, Water atomization, Powder size distribution, Control.

2. Background

Powder size distribution is a critical powder property often neglected by water atomization researchers. However, it is vital for the competitiveness of powder metallurgy to come to terms, not only with averages, but also with variations such as the size distribution.

A wide size distribution has one advantage; it will yield a powder with a high filling density since smaller particles may seep through the network formed by larger ones.

From a quality standpoint, this is negative, since a consequence of the ability of small particles to seep between larger ones, is powder separation; all handling of the powder will risk the homogeneity of the powder. In a filled volume for example, we would find smaller fractions in the bottom and central parts. A consequence is that the part may densify inhomogeneously due to the different sintering activities. Distortion and mechanical property problems will follow. The smallest particle sizes are unwanted in press and sinter operations for several reasons. The smallest particle sizes may lead to excessive dusting. Dusts of pyrophoric metals ignite easily, but even less reactive metal dusts should be handled with care. Dust of toxic metals does also pose a health hazard. Powders smaller than 10 μm may reach the lungs and be uptaken by the body.[1] Since small particles may slip between the tool clearances and cause problems in terms of cold welding, particle sizes smaller than 20 microns are generally unwanted for PM steel applications. More complicated part designs often require multi level tooling, and in such cases clearances may add up to 50 microns, sharpening the powder quality requirements even further. At the other end of the scale, large particles reduce sinterability and impair surface finish.

Iron powder producers often top off the size distribution with 100 (150-μm opening) mesh sieves to eliminate large particles. Cyclone separation may be used to eliminate the smallest ones. Even if the separated material could be sold to other applications, the remaining size distribution would be a mix between a square and a lognormal one; that is with more powder in the tails and thus more prone to segregate. The best solution is to produce powder with a narrow and precise size distribution.

One way to narrow the size distribution would be to redesign the atomizing facility, to change chamber atmosphere, to change the composition of the melt, or to increase the superheat.[2-4]

Another way to reduce variation would be to avoid that the states of the atomization variables are different from batch-to-batch, and during ongoing atomization. Many of the inherent variables of water atomization are currently not suited for on-line control due to the difficulties in monitoring the process. One way to come to terms with this would be to reduce the sensitivity of the process versus non-controlled variation. The goal of this investigation is to illuminate some factors that may influence size distributions and to suggest means to reduce the influence of these.

2.1 Modeled Process:

First, consider a 15kg laboratory atomizer, set up for iron powder manufacture, Figure 1a. The metal is melted in a bottom-emptied induction furnace, where the stopper-rod contains a thermocouple. While the scrap melts, the tundish is preheated with gas burners. At the predetermined temperature, the stopper-rod is lifted and the melt pours through a nozzle into a pre-heated tundish. As soon as the melt enters the tundish, some of the melts seep through a second nozzle into the atomization zone. Water jets then granulate the melt stream into droplets, which rapidly solidify into iron powder.

During atomization, the liquid iron is poured via a tundish in a free-fall arrangement. The size of the metal orifice, together with the tundish metal head control the metal flow. The water orifice setup controls the impacting angle between the water jet and liquid metal stream, and water velocity. Empirical results from a similar arrangement have been presented by Bergquist[4].

Next, consider a 50-ton plant. Some differences versus the small facility are as follows. The melt is produced in a separate melting facility and kept in the ladle between melting and atomization. The ladle does not contain heating possibilities. The level of the melt in the tundish is kept constant by visual inspection and is adjusted by changing melt flow from the ladle. During ongoing atomization, the powder slurry is continuously pumped off and dewatered. The water is then reused to atomize the melt.

Similar to the laboratory facility, the tundish is heated by gas burners before atomization.

2.2 Model of Small Facility:

The model considers the flow, surface tension and viscosity of the melt, and these properties are connected to an atomization model. (The models were implemented in MATLAB software).

2.2.1 Melt Flow

The liquid velocity, u, of a liquid flowing out of a container into open air follows Torricelli's law:

$$u(t)=\phi\sqrt{2gh(t)} \tag{1}$$

where t is time, ϕ is a constant between zero and one and one referring to ideal frictionless flow, g is the gravity and h is head of the liquid. The formula is valid for situations where the nozzle is short enough so that the velocity profile is negligible, which is the case considered here.

The volume of the melt in the furnace crucible, or ladle, is written (the ladle is a cylinder with bottom area A_1, and a nozzle with area a_1, V^0 is the volume of the volume of the molten metal):

$$V_1 = \frac{A_1}{4}\left(2\sqrt{\frac{V^0}{A_1}} - \phi\frac{a_1\sqrt{2gt}}{A_1}\right) \quad (2)$$

As soon as the melt starts to flow into the tundish, melt will pass through to the atomization zone. The iron flow out of the furnace is highest at the start, and is reduced as the ferrostatic pressure drops. From the tundish, the initial flow is low since ferrostatic pressure is low, but it picks up to a maximum, and then decreases to zero.

With initial conditions as in Table I, the volumes of ladle and tundish as a function of time are seen in Figure 2a. The area of the tundish covered by melt as a function of time is seen in Figure 2b. (Compared to experiments performed by Bergquist[4], the assumption that the tundish has a cylindrical form is a simplification; the shape of the tundish bottom in the facility used by Bergquist is semi-hemispherical. For simulations, it is also assumed that the exit hole of the tundish is at the tundish bottom, whereas the actual tundish has a conical nozzle entry and the minimum diameter was located below tundish bottom level). The speed of the water jets, u_w, can similarly be estimated as $u_w = \phi_w\sqrt{\frac{2p_w}{\rho_w}}$, where p_W is the water pressure, and ρ_W is the water density.

2.2.2 Heat flow

The temperature at atomization depends on the temperature of the melt in the ladle, and how much the melt cools down before atomization. The pre-heated graphite tundish has an initial temperature of 900°C. As soon as the melt hits the tundish, heat starts to flow from the melt into the tundish by conduction, and also through radiation from the free surface of the melt.

If V_2 is the control volume [m^3], ρ_{Me} is the density of the melt [kg m^{-3}], C_P is the heat capacity [J kg^1 K^{-1}], T is the temperature [K], and t is the time [s], then the heat of the melt flowing into and out of the control volume (tundish) may be expressed as:

$$\dot{q}_{LMe,in} = C_P\rho_{Me}T_1\dot{V}_{2in} \quad (3)$$

$$\dot{q}_{LMe,out} = C_P\rho_{Me}T_2\dot{V}_{2out} \quad (4)$$

where $\dot{q}_{LMe,in}$ and $\dot{q}_{LMe,out}$ is the heat flow into and out of the control volume [J/s], $\dot{V}_{2in}$ and $\dot{V}_{2out}$ are the melt flow into and out of the control volume [m3/s].

The convective heat flow through a surface into an infinite body subjected to a transient temperature change may be written as eq. 5:[5]

$$\dot{q}_C = k_c A\frac{(T_s - T_i)}{\sqrt{\pi\alpha t}} \quad (5)$$

where T_i and T_s are initial body temperature and surface temperature [K], k_c is the thermal conductivity [W m^{-1} K^{-1}], A is the area of the interface [m^3], α is thermal diffusivity, $\alpha = k_c/(\rho C_P)$ [m^2 s^{-1}] where ρ is the density [kg/m^3], C_P is the heat capacity [J $kg^{-1}K^{-1}$].

Heat flow by radiation from a gray surface, with area A_1 [m^2] and emissive index ε at a temperature T_1 to the surrounding black enclosure with temperature T_2 follows:

$$\dot{q}_R = A_1 \varepsilon_1 \sigma \left(T_1^4 - T_2^4 \right) \tag{6}$$

With some simplifications and assumptions, equations (3) to (6) are used to calculate temperature of the tundish melt. The simplifications are as follows: the tundish thickness is considered infinite. One dimensional heat flow is assumed. It is assumed that the temperature of the inner surface of the tundish in contact with the melt has the same temperature as the melt. It is assumed that the temperature profile through the tundish walls is equal wherever the tundish is in contact with the melt. Elsewhere the temperature of the tundish walls is assumed to have the same temperature as when atomization started. It is also assumed that the temperature of the melt is equal throughout the tundish volume. The free melt surface is assumed to radiate versus a black body surface with constant temperature equal to initial tundish volume. It is also assumed that as soon as the melt reaches the solidus temperature, freezing starts and heat of fusion is released. Finally, it is assumed that the temperature of the melt flowing into the tundish has constant temperature during the atomization.

Take the tundish inner volume as a control volume. Heat flowing into the tundish by the melt must balance accumulated heat within the tundish and heat flowing out. An energy balance taken over the internal volume of the tundish is written as:

$$\int_0^t (\dot{q}_{LMe,in}(t) + \dot{q}_{LMe,out}(t,T) + \dot{q}_{C,TD}(t,T) + \dot{q}_R(t,T))dt + Q_{LMeTD}(t,T) + Q_{SMeTD}(t,T) = 0 \tag{7}$$

where $\dot{q}_{LMe,in}$ is the heat flowing into the control volume by incoming melt [J/s], $\dot{q}_{LMe,out}$ is the heat flowing into the tundish by out-flowing melt [J/s], $\dot{q}_{C,TD}$ is the convective heat flowing into the control volume [J/s], $\dot{q}_{R,TD}$ is the heat radiation flowing in to the control volume [J/s]. Q_{LMeTD} is the heat accumulated in the melt of the control volume, and Q_{SMeTD} is the heat accumulated in the solidified melt in the control volume [J].

The tundish temperature is expressed as:

$$T = \begin{cases} Q_{LSMeTD} / (C_p \rho V_2), & Q_{SMeTD} / (C_p \rho V_2) > T_m \\ T_m, & Q_{SMeTD} / (C_p \rho V_2) < T_m \end{cases} \tag{8}$$

where T_m is the solidus temperature [K]. With these assumptions and simplifications, the tundish temperature equation was solved numerically. The simulated tundish temperature as a function of time for two melts, one started at 1590°C, the other started at 1730°C with other conditions as in Table 1 is shown in Figure 3. The rapid decrease in temperature during final atomization reflects the small melt volume in the tundish, and no hot melt flowing into the tundish from the furnace. The plateau at the end of the atomization comes from melt starting to freeze.

2.2.3 Models of Physical Properties of the Melt

The energy required to create new surface area when a liquid is disintegrated into droplets is directly related to the surface tension of the liquid. For this reason, surface active elements, which reduce surface tension would also play a role.[6] Results of recent experiments (ref. [4]) suggest that external oxygen present already lowers surface tension considerably, and that the effects of surface active impurities are visible only for additions large enough to lower surface tension even further.

Surface tension has a negative temperature coefficient of a pure iron melt. Binary iron-surfactant (for instance Fe-O) melts exhibit a positive coefficient in surface tension measurement equipment. This is since surfactants evaporate. Such a mechanism is unlikely during water atomization; instead, oxygen

pick-up is to be expected. Oxygen, the major surface-active element during water atomization, is present in the water and the gas of the water jets and can react with the iron. Neither was an increase in surface tension as a function of increased melt temperature seen by Bergquist.[4]

A model for surface tension was therefore created where the positive temperature effect was ignored. Surface tension instead follows the behavior of a pure melt,[6] however reduced for high oxygen content.

$$\gamma_{Me} = c(2.46 - 0.00034\,T) \tag{9}$$

where γ_{Me} is the surface tension [N/m], c is a constant due to oxygen coverage; c equals 0.7 in the calculations, and T is the melt temperature in K.

The viscosity, ν, of the melt is assumed to be unaffected by small amounts of solute, and is a function of temperature, eq. (10).

$$\nu_{Me} = \nu_{0,Me} e^{E/(RT)} \tag{10}$$

where E is the activation energy, for iron E = 41.4E3 J/mol, ν_0 = 370 Ns/m^2, R is the gas constant, 8.3144 J /(mol K).[7] In Figure 4, the surface tension and viscosity behaviors versus temperature are seen according to these models.

2.2.4 Water Atomization Model

To model how shifts of the states of a process-variable may influence the particle size, a good formula for the atomization must be used. For gas atomization, several similar ones have been proposed; this is not the case for water atomization. Gas atomization has been more thoroughly investigated, partly because of larger research funding, partly because of the relative simplicity of studying gas atomization in situ.

In a work by Bergquist, an empirical model, eq. (11), for resulting particle size from water atomization was proposed.[4] This model is used in current simulations.

$$\mu P = k \frac{\gamma_{Me}^{0.8} \nu_{Me}}{p_w^{0.8} \sin\alpha} \left(\frac{G_W}{G_{Me}} \right)^{-0.043} \tag{11}$$

where μP is the median particle size, G_{Me} and G_D are mass flow of melt and water respectively, p_w is the water pressure, and k is a constant with units m$^{0.2}$N^{-1}s^{-1}.

2.3 Simulated Conditions:

In Table I, the conditions used for laboratory facility simulations are found.

3. Results

3.1 Variation sources affecting particle size during an atomization run

3.1.1 Small facility

The constant k in Table I was calibrated versus results from Bergquist [4]. The experimental conditions of each run were simulated, and the average simulated particle size versus measured particle size is shown in Figure 5. (In the paper, it was suggested that the surface tension of run F102 was 30% lower due to addition of 1.5 w/o S. The surface tension model was adjusted accordingly). The correlation between simulated and measured particle sizes is 0.94. The simulation does underestimate the range of the medium particle size results of the experiment, and this is mostly due to the larger influence of

water pressure seen in ref. [4] compared to the corresponding exponent in equation 11. It is also due to the conservative estimate of the viscosity exponent.

Figure 6 shows the resulting particle size of an atomization run. The low melt flow combined with high melt temperature results in small particle sizes in the beginning of a run. As the temperature drop accelerates, particle sizes grow. As solidification starts, particle sizes are reduced due to reduced flows.

The standard deviations of particle sizes from melts heated to temperatures between 1590 to 1730°C were investigated for the small facility. This standard deviation was not the same as the usual lognormal standard deviation. Instead, the average particle size result of eq. 11 was multiplied by the melt flow during each time-step of the simulation. After a completed atomization run, the particle sizes and volumes produced during each time-step were summed into a distribution of average particle sizes. This distribution was then used to calculate average particle size and standard deviation. The model results suggested that the standard deviations would increase with increased superheating. In Figure 7, the relative standard deviation is plotted versus the melt temperature. (The relative standard deviation is the standard deviation divided by the average particle size during an atomization.

3.1.2 Large Facility:

Tundish temperature was measured during atomization of six 50-ton batches at an iron-powder atomization-facility. An average temperature curve is seen in Figure 8. This temperature curve was fed into the water atomization model and the simulated powder size for this run is seen in Figure 8. It was assumed that flow of both iron and water was constant. The particle size median deviates on the average 2% around target during such an atomization.

3.2 Variation Sources Affecting Particle Size Between Batches:

3.2.1 Large facility

100.000 industrial atomization runs were simulated with a temperature normally distributed with a mean of 1700°C and a standard deviation of 20°C, (or N(1700°,20°)), a figure obtained from logged process data. The result of the simulation showed that the mean particle size of each atomization varied with a standard deviation of 3% around target. These temperature variations may result from different initial heating temperatures of the melt, but also from difference in queuing times for melts to be atomized.

The ferrostatic pressure and thus the melt flow is controlled manually. If the ferrostatic head of the tundish can be assumed to vary with a standard deviation of 5cm around the target of 0.5m (N(0.5m,0.05m)), and this variation is taken together with the temperature variation, the resulting particle size will be off target by 3.2% on the average.

4. Discussion

4.1 Flow Model:

Simulated atomization times were 43s for the laboratory simulations compared to the 30-36s measured during the experimental atomizations. The hemispherical shape of the tundish but also the conical nozzle is adding ferrostatic pressure over the nozzle exit and this should account for the difference.

4.2 Heat Flow Model:

The heat flow model predicts that some melt will start to freeze in the tundish during the laboratory atomizations (0.8g). Compared to actual atomizations, the heat extraction rate estimate made here is probably a conservative estimate, although the actual atomization times were shorter.. The actual atomizations always left metal residue, or small freeze-ups.

Atomization" Powder Metallurgy, *43(1), 37-42*.

Robust design means setting the process parameters so that the process is less sensitive to variation. Simulations with different superheatings for the laboratory scale plant showed a more stable powder size for low superheating, because of the more stable tundish temperatures. This is contrary to what is found experimentally.[2, 4] In Figure 9, the experimental results from Bergquist[4] regarding particle size standard deviation are shown. Although the conflicting results at first seem to invalidate the whole model, it instead shows that there are two opposing mechanisms of temperature. The modeled effect that lower superheating would lead to a narrowed particle size distribution is reasonable, since temperatures of the melt in the tundish, and thus melt properties are more stable with lower superheats. The agreement with the experimental median particle sizes of ref.[4] also shows that the model is partially correct.

The opposing mechanism responsible for the narrowed particle size distribution seen experimentally with high superheatings may be related to the solidification of the droplets. The solidification rate for large droplets is lower than for small ones. As large particles have longer solidification times, the probability is higher that they will be subsequently split into smaller particles; thus narrowing size distribution. The more prolonged solidification times expected for droplets originating from melts with high superheatings might strengthen this effect. A more complete water atomization model should consider the disintegration mechanism.

Heating the tundish to a higher temperature before atomization would result in lower variation due to smaller temperature fluctuation during ongoing atomization. The metal flow rate has some importance, and powder producers may study how this could be kept constant. One stabilizing feature would be to design the tundish so that the melt head is not sensitive versus the volume of the melt in the tundish. Since flow is proportional to the square of melt head, a stabilizing possibility of melt flow due to differences in melt head would be to increase total melt head.

5. Conclusions

The particle size distribution is partly a function of variations during an atomization and of variations occurring between batches. Melt temperature in particular, but also melt flow should be controlled to minimize variation. It is also suggested that the narrowed particle size distributions seen experimentally for high superheatings are related to a prolonged solidification.

The simulation also shows when freeze-ups of the tundish are to be expected, and one application of simulation would be for predictive purposes during processing.

6. Summary

Simulations were used to investigate the water atomization process for iron powder production. The model was based on empirical models for surface tension, viscosity and water atomization, and physical models for flow and temperature transfer.

Two sizes of atomization facilities were studied, a 15kg unit and a 50ton unit. The model predictions suggest that both facilities should strive for constant temperature of the melt during atomization.

Simulations showed that higher superheatings would increase powder size variation of a laboratory atomizer, and this was opposed to experimental results, ref. [4]. The different behavior was attributed to two opposing mechanisms active during atomization.

7. Acknowledgements

The project has been financed by the Swedish National Board for Industrial and Technical Development, NUTEK, under grants # 95-06473 and 95-11037. Thanks to Björn Haase, Höganäs AB, for temperature measurements, for process estimations and for comments on the work. Thanks also to Anita Köhler-Hanno for proofreading the manuscript.

Atomization" Powder Metallurgy, *43(1), 37-42*.

Atomization" Powder Metallurgy, *43(1), 37-42*.

8. References

1 R.M. GERMAN: "Powder Metallurgy Science", 2nd edn, 1994, Princeton, NJ, USA, Metal Powder Industries Federation.

2 T. TAKEDA and K. MINAGAWA: "Effects of Atmosphere During Water Atomization on Properties of Copper Powders", *J. Jpn. Soc. Powder Metall.*, 1978, **25**, (7), 1-6.

3 J.J. DUNKLEY: "Atomization", Metals Handbook, Vol. 7 - Powder Metallurgy, 10th edn., (ed. W.B. Eisen et al.), 35-52, 1998, Materials Park, American Society for Metals.

4 B. BERGQUIST: "New insights into water atomization of iron regarding influencing variables", *to apperar in Powder Metall.*, 1999,

5 F. KREITH and M.S. BOHN: "Principles of Heat Transfer", 1986, Harper & Row, Publishers, New York, NY, USA.

6 B.J. KEENE: "A Survey of Extant Data for the Surface Tension of Molten Iron and its Binary Alloys", NPL Report DMA(A) 67, National Physical Labs, Teddington, Middlesex, UK, 1983.

7 C.J. SMITHELLS: "Smithells Metals Reference Book", 7th edn, (ed. E. A. Brandes and G. B. Brook), 14-16--14-17, 1992, Oxford, Butterworth-Heinemann.

8 A.J. YULE and J.J. DUNKLEY: "Atomization of melts", 1994, Oxford, Oxford University Press.

9 O. KUBASCHEWSKI and C.B. ALCOCK: "Metallurgical Thermo- Chemistry", 5:th edn., 1979, Toronto, Pergamon Press.

10 F.W. SCHMIDT, R.E. HENDERSON and C.H. WOLGEMUTH: "Introduction to Thermal Science - Thermodynamics; Fluid Dynamics; Heat Transfer", Second edn., 1993, New York, John Whiley & Sons.

Table I. Conditions used During Laboratory Scale Simulations

Atomized metal	Fe, 0.4w/o C
Freezing temperature, T_M	1505°C
Atomized amount, m	7kg
Liquid metal emissive index, ε	0.5
Thermal capacity of liquid metal $C_{P,L}$	746J kg^{-1} K^{-1}
Density of liquid metal ρ_L	7030kg m^3 (ref. [8])
Latent heat of fusion, iron, Δh_f	246kJ kg^{-1} (ref. [9])
Flow friction constant, ϕ	0.98
Ladle radius, R_L	55.25mm
Ladle nozzle radius, r_L	4.2mm
Tundish radius, R_T	45mm
Tundish nozzle radius, r_T	3.2mm
Tundish pre-heat temperature, T_0	900 °C
Thermal capacity of tundish material (anthracite) $C_{P,TD}$	1260J kg^{-1} K^{-1} (ref. [10])
Density of tundish material, ρ_{TD}	1260kg m^{-3} (ref. [10])
Heat conductivity of tundish material, $k_{C,TD}$	0.26W m^{-1} K^{-1} (ref. [10])
Water flow, Q_w	0.92kg/s
Apex angle, α	25°
Water pressure, p_W	15MPa
Formula constant, k	7900$m^{0.2}N^{-1}s^{-1}$

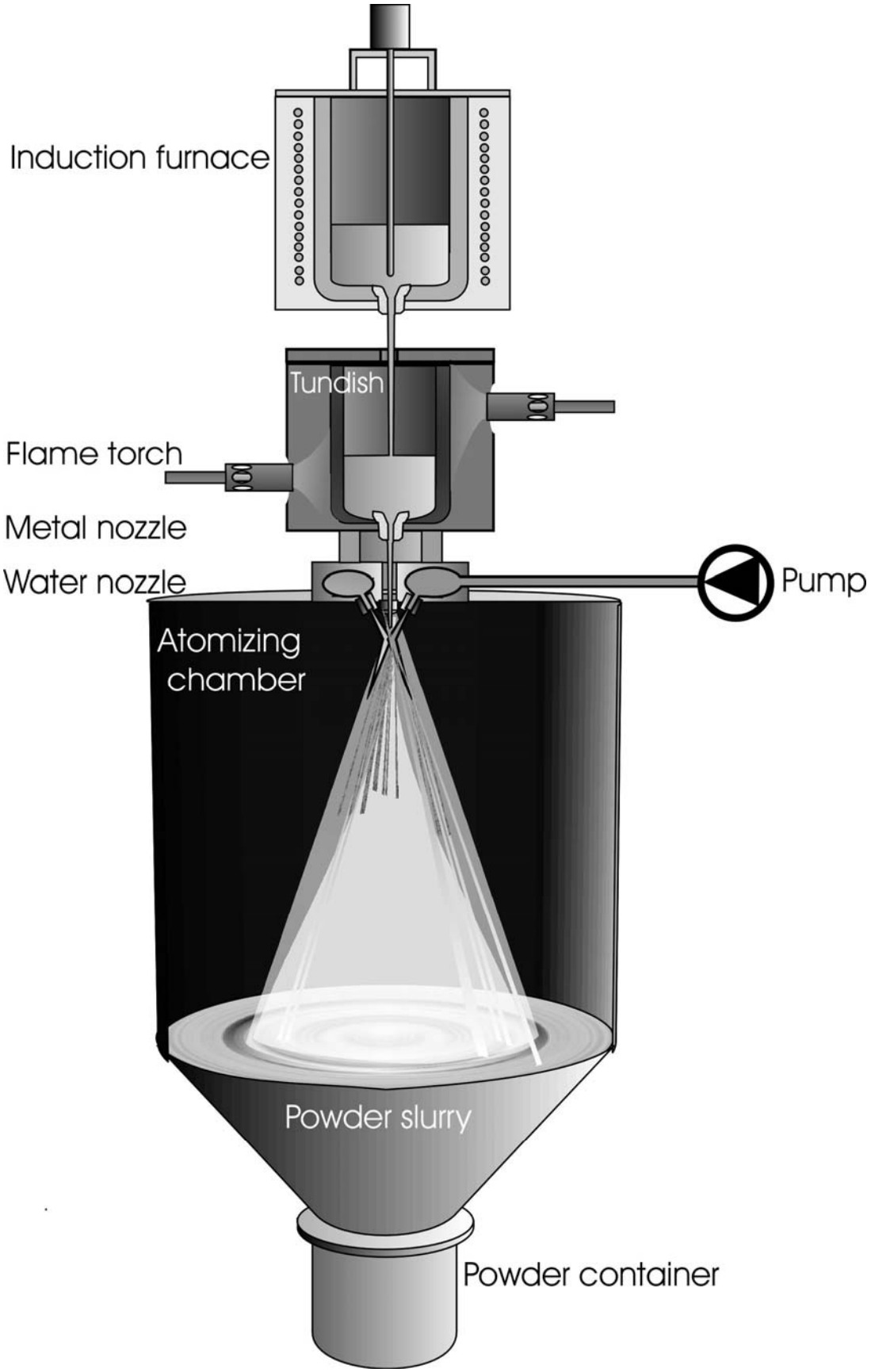

Figure 1a. *Small atomization facility.*

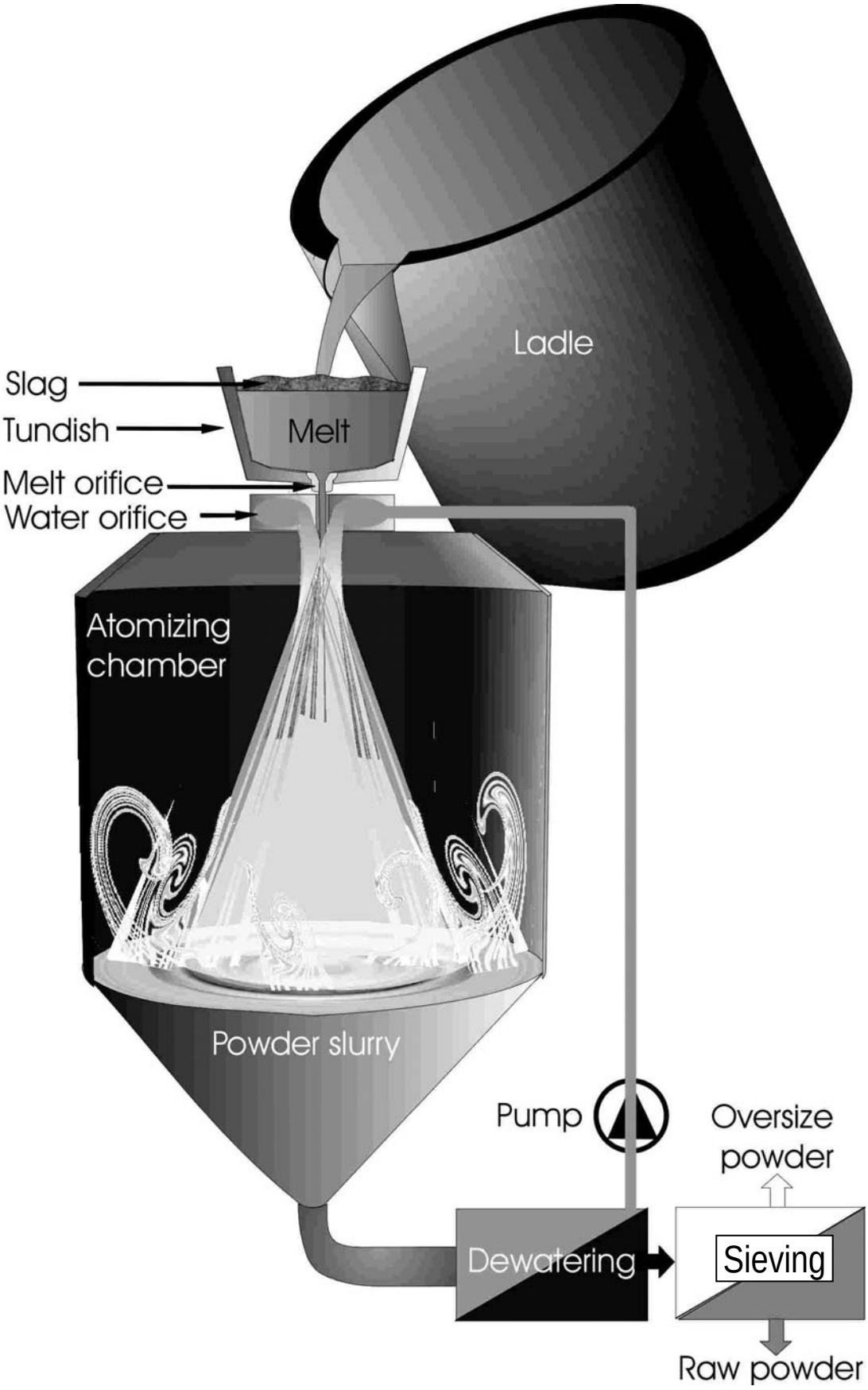

Figure 1b. *Large atomization facility.*

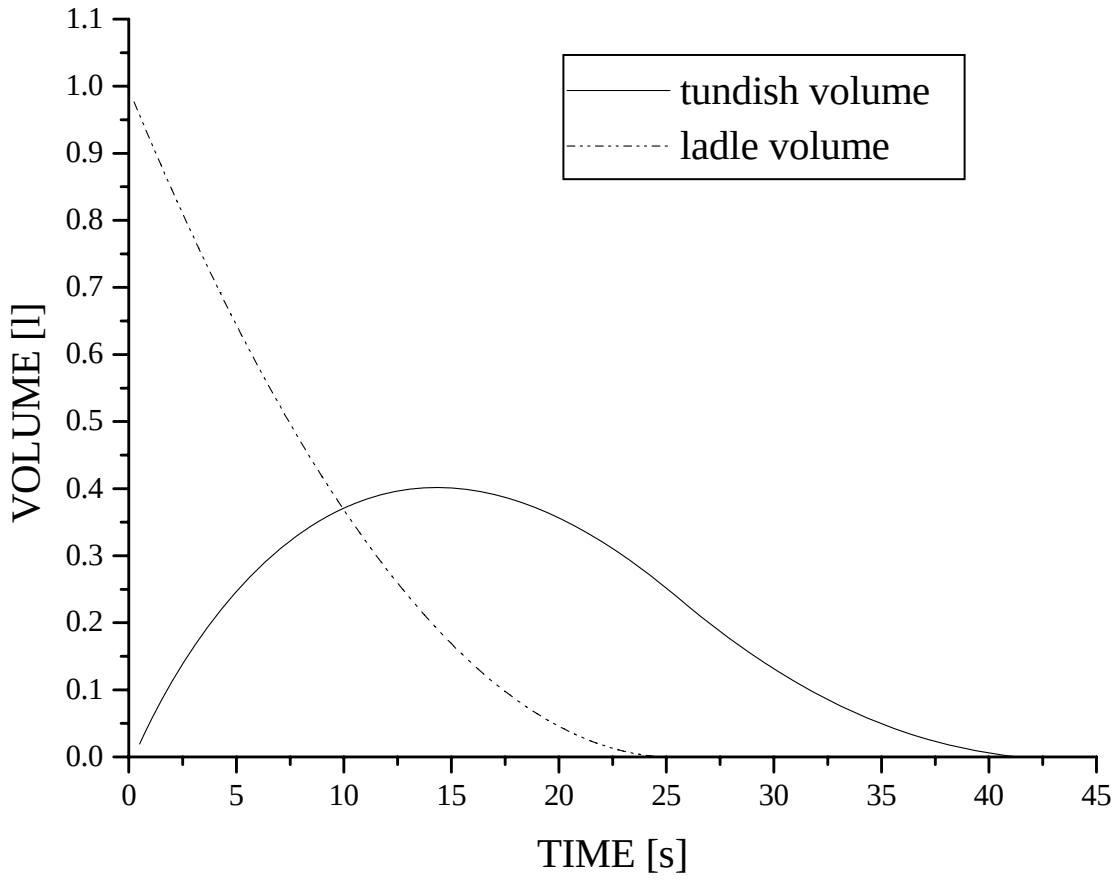

Figure 2a. *Melt volume of ladle and tundish as a function of time (simulation).*

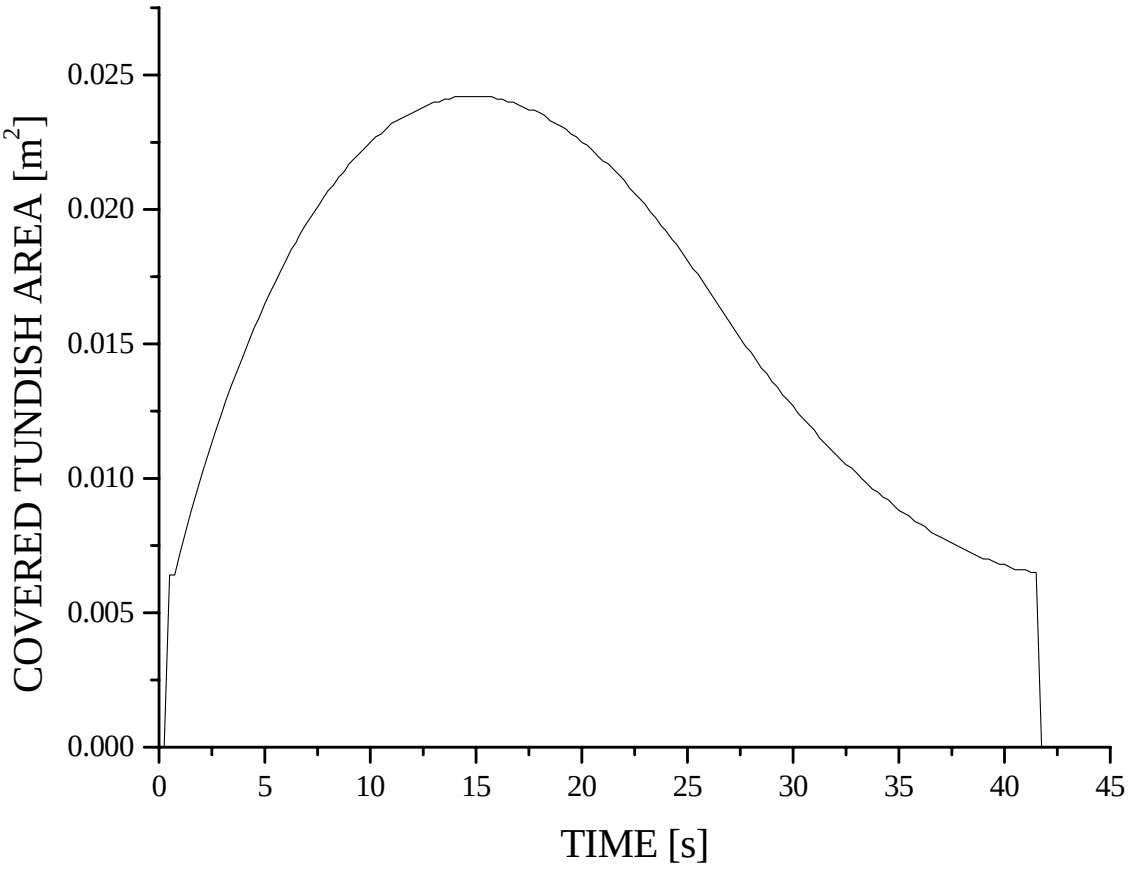

Figure 2b. *Covered tundish area as a function of time (simulation).*

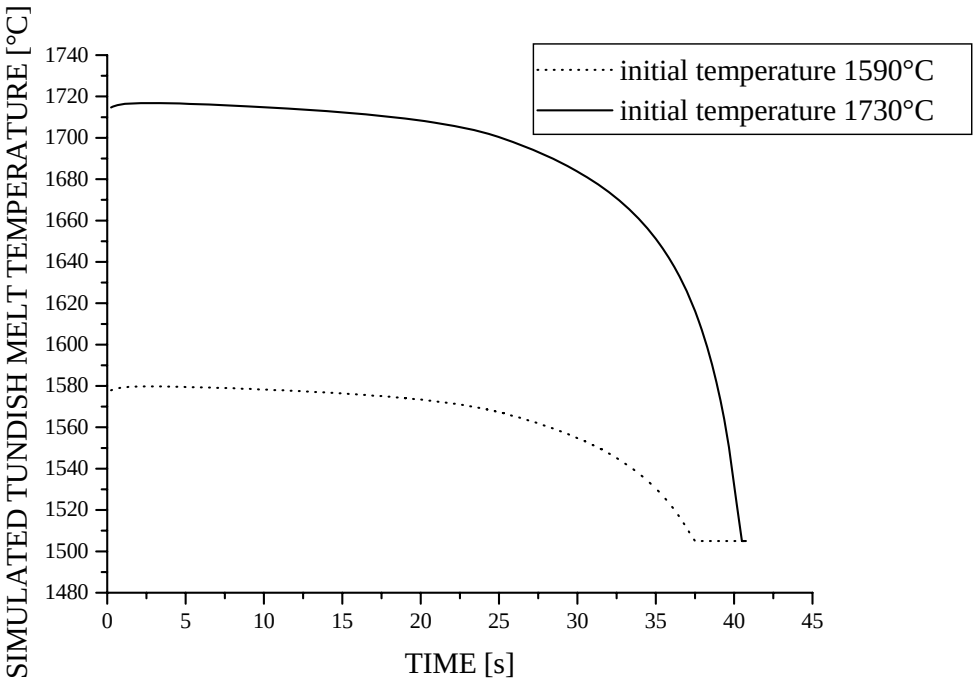

Figure 3. *Tundish melt temperature as a function of time (simulation).*

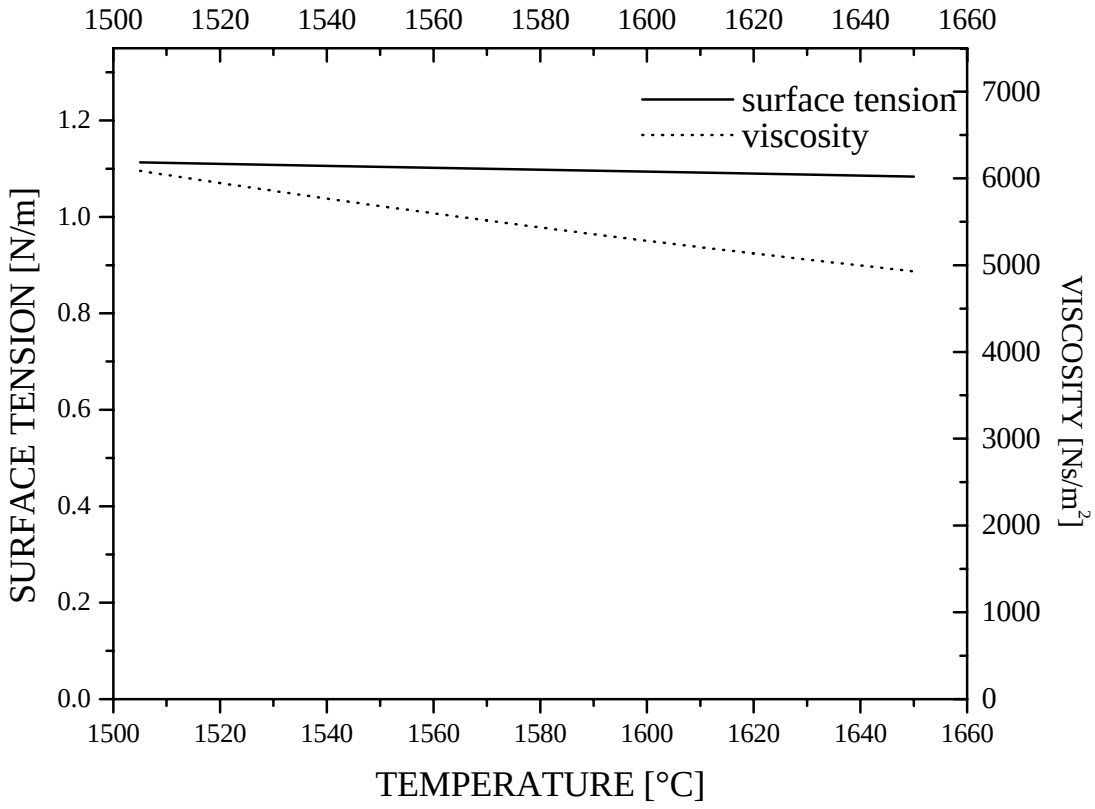

Figure 4. *Surface tension and viscosity according to model versus temperature.*

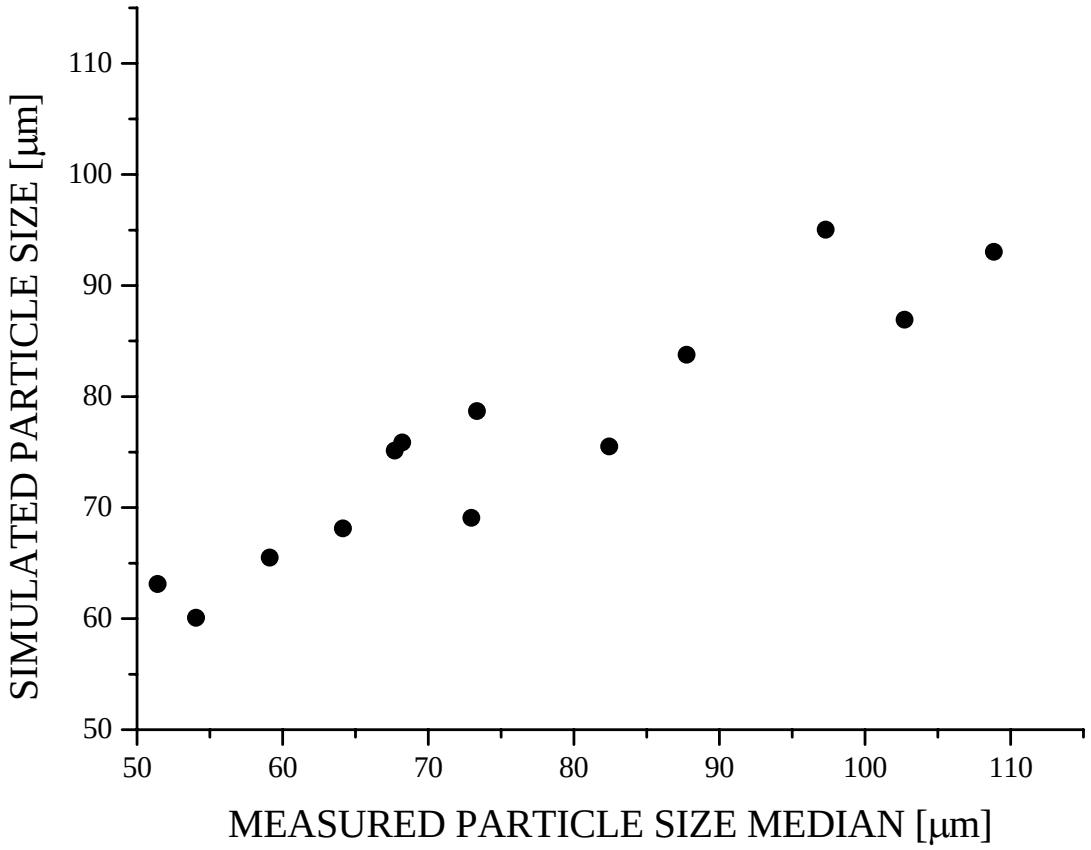

Figure 5. *Simulated particle size versus measured particle size from ref. [4].*

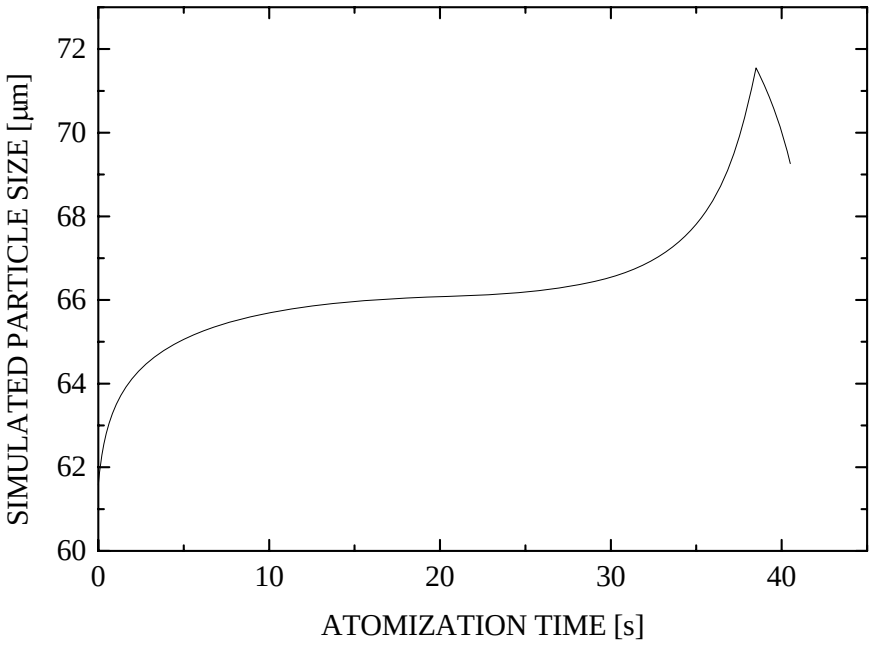

Figure 6. *Resulting particle size during a laboratory atomization run (simulation).*

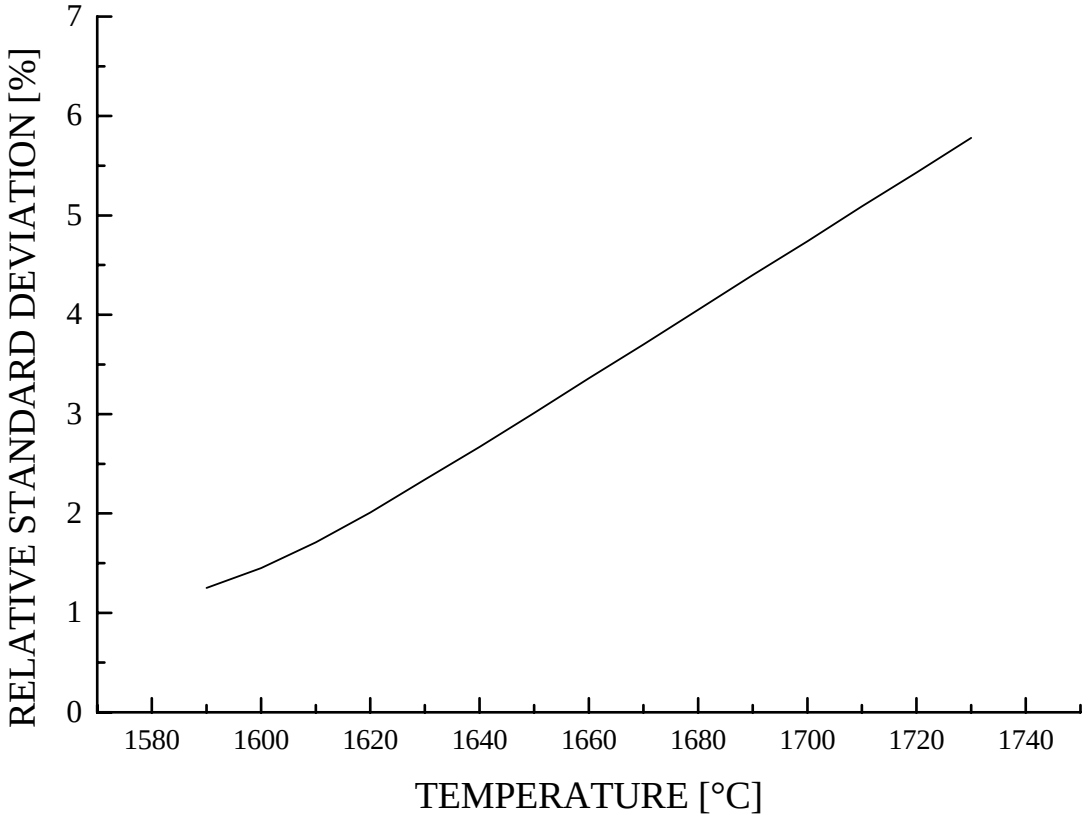

Figure 7. *Relative standard deviation versus melt temperature (simulation).*

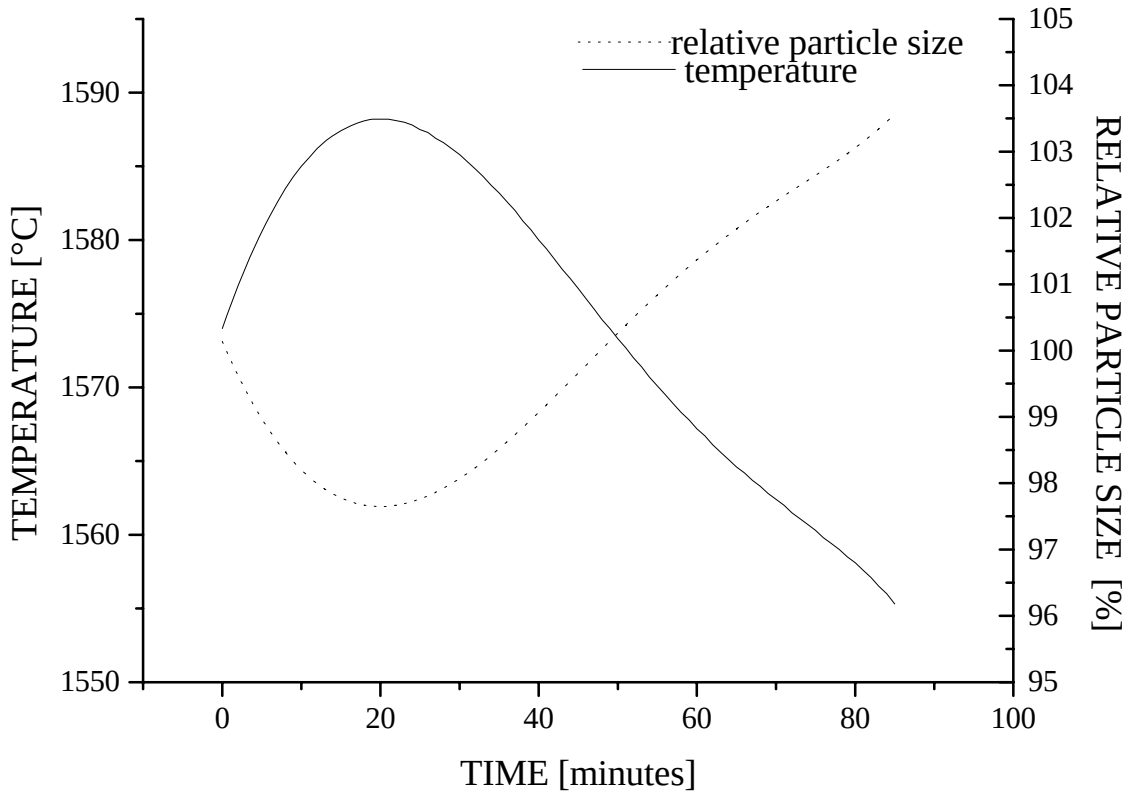

Figure 8. *Measured tundish temperature and calculated particle size during an atomization of an industrial batch.*

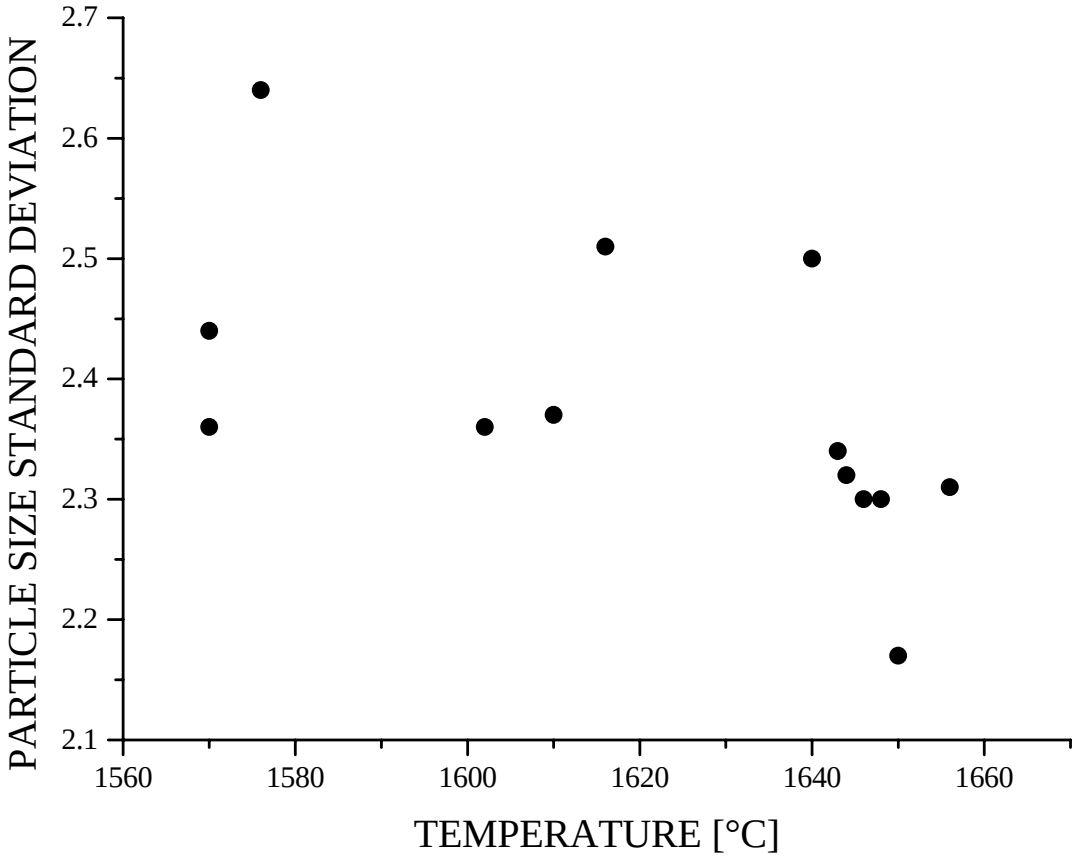

Figure 9. *Measured particle size standard deviation versus. temperature (from ref.[4]).*